



Contents lists available at ScienceDirect

Deep-Sea Research II

journal homepage: www.elsevier.com/locate/dsr2

Particle export within cyclonic Hawaiian lee eddies derived from ^{210}Pb – ^{210}Po disequilibrium

E. Verdeny^{a,*}, P. Masqué^{a,b}, K. Maiti^c, J. Garcia-Orellana^{a,b}, J.M. Bruach^a,
C. Mahaffey^d, C.R. Benitez-Nelson^{c,e}

^a Departament de Física, Universitat Autònoma de Barcelona, 08193 Bellaterra, Spain

^b Institut de Ciència i Tecnologia Ambientals, Universitat Autònoma de Barcelona, 08193 Bellaterra, Spain

^c Department of Geological Sciences, University of South Carolina, Columbia, SC 29208, USA

^d Department of Oceanography, SOEST, University of Hawaii, Honolulu, HI 96822, USA

^e Marine Science Program, University of South Carolina, Columbia, SC 29208, USA

ARTICLE INFO

Article history:

Accepted 6 February 2008

Available online 15 May 2008

Keywords:

Carbon export

Polonium

Lead

Mesoscale eddies

Hawaiian Islands

ABSTRACT

Particle export from the upper waters of the oligotrophic ocean may play a crucial role in the global carbon cycle. Mesoscale eddies have been hypothesized to inject new nutrients into oligotrophic surface waters, thereby increasing new production and particle export in otherwise nutrient deficient regimes. The E-Flux Program was a large multidisciplinary project designed to investigate the physical, biological and biogeochemical characteristics of cold-core cyclonic eddies that form in the lee of the Hawaiian Islands. There, we investigated particle dynamics using ^{210}Pb – ^{210}Po disequilibrium. Seawater samples for ^{210}Pb and ^{210}Po were collected both within (IN) and outside (OUT) of two cyclones, *Noah* and *Opal*, at different stages of their evolution as well as from the eddy generation region. Particulate carbon (PC), particulate nitrogen (PN) and biogenic silica (bSiO₂) export fluxes were determined using water-column PC, PN, and bSiO₂ inventories and the residence times of ^{210}Po . PC and PN fluxes at 150 m ranged from 1.58 ± 0.10 to 1.71 ± 0.16 mmol C m⁻² d⁻¹ and 0.22 ± 0.02 to 0.30 ± 0.02 mmol N m⁻² d⁻¹ within Cyclones *Opal* and *Noah*. PC and PN fluxes at OUT stations sampled during both cruises were of similar magnitudes, 1.69 ± 0.16 to 1.67 ± 0.16 mmol C m⁻² d⁻¹ and 0.30 ± 0.03 to 0.26 ± 0.03 mmol N m⁻² d⁻¹. The bSiO₂ fluxes within Cyclone *Opal* were 0.157 ± 0.010 mmol Si m⁻² d⁻¹ versus 0.025 ± 0.002 mmol Si m⁻² d⁻¹ at OUT stations. These results of minimal PC and PN export, but significant eddy-induced bSiO₂ fluxes, agree very well with other studies that used a variety of direct and indirect methods. Thus, our results suggest that using elemental inventories and residence times of ^{210}Po is another independent and robust method for determining particle export and should be investigated more fully.

© 2008 Published by Elsevier Ltd.

1. Introduction

Particle export from the upper ocean plays a crucial role in the global carbon cycle (e.g., Sarmiento and Toggweiler, 1984). Within the open ocean, particle export occurs primarily through the “biological pump”, the uptake of carbon dioxide by phytoplankton and the subsequent formation of particles via zooplankton grazing, fecal pellet production, and a number of other biologically mediated processes (Volk and Hoffert, 1985; Ducklow et al., 2001). In the oligotrophic ocean, biological production is typically limited by major nutrients (N, P, Si) or trace metals (Fe), whose availability mostly depends on intense recycling within the euphotic zone. Only a small fraction is supported by external inputs, such as atmospheric deposition or upwelling of nutrient-rich waters from below.

In a steady-state ocean, these “new” nutrients set an upper limit for the amount of biologically fixed carbon that can be sequestered in deeper waters and hence the strength of the biological pump (Dugdale and Goering, 1967; Jenkins, 1988).

Recent studies suggest that mesoscale eddies may play a major role in facilitating new production and particle export in otherwise nutrient deficient waters by bringing nutrient-rich deep waters into the surface (Falkowski et al., 1991; McGillicuddy et al., 1998; Williams and Follows, 2003). This hypothesis remains controversial, however, given the few studies that have directly measured either new production or particle export in these ephemeral phenomena (Oschlies, 2001). In 2004 and 2005, a large multidisciplinary project, E-Flux, investigated the physical, biological and biogeochemical characteristics of cold-core cyclonic eddies that form in the lee of the Hawaiian Islands (Benitez-Nelson et al., 2007).

The E-Flux sampling scheme consisted of three 18-day sampling cruises that occurred within a 6-month sampling period. These cruises sampled two distinct mesoscale eddies during

* Corresponding author. Tel.: +34 93 581 1191; fax: +34 93 581 2155.

E-mail address: elisabet.verdeny@uab.cat (E. Verdeny).

different physical and biological stages of their evolution with Cyclone *Noah* sampled during E-Flux I (4–22 November 2004) and Cyclone *Opal* sampled during E-Flux III (10–28 March 2005) (Dickey et al., 2008; Kuwahara et al., 2008; Nencioli et al., 2008). E-Flux II (10–28 January 2005) sampled waters from an eddy generation region. Here, we focus on measurements of particle flux using the ^{210}Pb – ^{210}Po disequilibria.

^{210}Pb ($T_{1/2} = 22.3$ yr) and ^{210}Po ($T_{1/2} = 138.4$ d) are particle-reactive radioisotopes within the Uranium-238 decay chain that can be used as tracers of particle cycling in the upper ocean (e.g., Cochran and Masqué, 2003). Both radioisotopes have a strong affinity for particles, but have different binding mechanisms. ^{210}Pb adsorbs on particle surfaces whereas ^{210}Po also becomes incorporated via biological activity into the cytoplasm of some species of phytoplankton (Fisher et al., 1983) and bacteria (Cherrier et al., 1995; La Rock et al., 1996); its partitioning is similar to that of protein and sulphur within the cell (Fisher et al., 1983; Stewart and Fisher, 2003a,b; Stewart et al., 2005). Thus, ^{210}Po is preferentially enriched in organic tissue and is efficiently assimilated by zooplankton (Heyraud et al., 1976; Fowler and Knauer, 1986; Cherry and Heyraud, 1988). These differences in biogeochemistry result in ^{210}Po being more efficiently removed from surface waters than ^{210}Pb via sinking particles. Hence, disequilibrium between the two radionuclides occurs when biological activity is high, and can be used to examine particle export in a similar manner to the more commonly used ^{234}Th / ^{238}U radioactive pair (Cochran and Masqué, 2003; Waples et al., 2006), but on timescales ranging from several months to a year (constrained by the half-life of ^{210}Po).

To date, there have been relatively few applications of the ^{210}Pb – ^{210}Po disequilibrium technique to determine carbon export in marine ecosystems (Shimmield et al., 1995; Friedrich and Rutgers van der Loeff, 2002; Murray et al., 2005; Stewart et al., 2007b; Buesseler et al., 2008; see Verdeny et al., 2008). Given the potentially long life times of mesoscale eddies (~9 months) as well as their rapid biogeochemical evolution, ^{210}Pb – ^{210}Po disequilibria appear as an ideal tracer of particle export within these systems. To our knowledge, this is one of the first measurements of ^{210}Pb – ^{210}Po disequilibria within mesoscale eddies, in parallel to the data reported in Buesseler et al. (2008) within the framework of the EDDIES program carried out in the Sargasso Sea.

2. Materials and methods

2.1. Sampling area and sample collection

Both cold-core and warm-core eddies of approximately 180 km in diameter are regularly generated by strong and persistent north-easterly trade winds that funnel through the Alenuihaha Channel that separates the islands of Maui and Hawaii (Patzert, 1969; Chavanne et al., 2002). In November 2004 (E-Flux I), January 2005 (E-Flux II) and March 2005 (E-Flux III), water samples for ^{210}Pb and ^{210}Po were collected in the lee of the Hawaiian Islands (Fig. 1). A detailed discussion of the hydrography of each of the field experiments, the sampling strategies and methods employed, as well as general observational results are found in companion papers by Dickey et al. (2008), Kuwahara et al. (2008) and Nencioli et al. (2008).

Prior to shipboard sampling, each eddy was located using satellite (MODIS and GOES) (see Fig. 2) derived sea-surface temperatures (SST). Cyclone *Noah* was identified in GOES SST imagery in 13–21 August 2004 (Kuwahara et al., 2008), and likely formed due to strong and persistent trade winds during that time period. Cyclone *Noah* remained in a relatively constant geographic location during sampling, to the west of the island of Hawaii. Direct biological and physical measurements during E-Flux I suggest that Cyclone *Noah* was in a spin-down or decay phase of its life cycle (Rii et al., 2008). During E-Flux II wake winds of variable direction dominated the sampling area. No mesoscale features were observed by satellite SST, consistent with the unfavourable wind conditions for the generation of mesoscale eddies during the preceding month. Samples were therefore collected in the region of eddy formation coincident with two-subsurface anomalies that may have been precursors of future eddies. During E-Flux III, strong north-easterly trade winds returned to the Alenuihaha Channel and produced a cold-core cyclonic eddy, Cyclone *Opal*, which became visible in satellite imagery between 18 and 25 February 2005 (Nencioli et al., 2008). The subsurface physical signal of Cyclone *Opal* as well as its biological community structure suggested that the eddy was a well-developed physical feature in the midst of a biological transition from large to small phytoplankton (Benitez-Nelson et al., 2007; Rii et al., 2008).

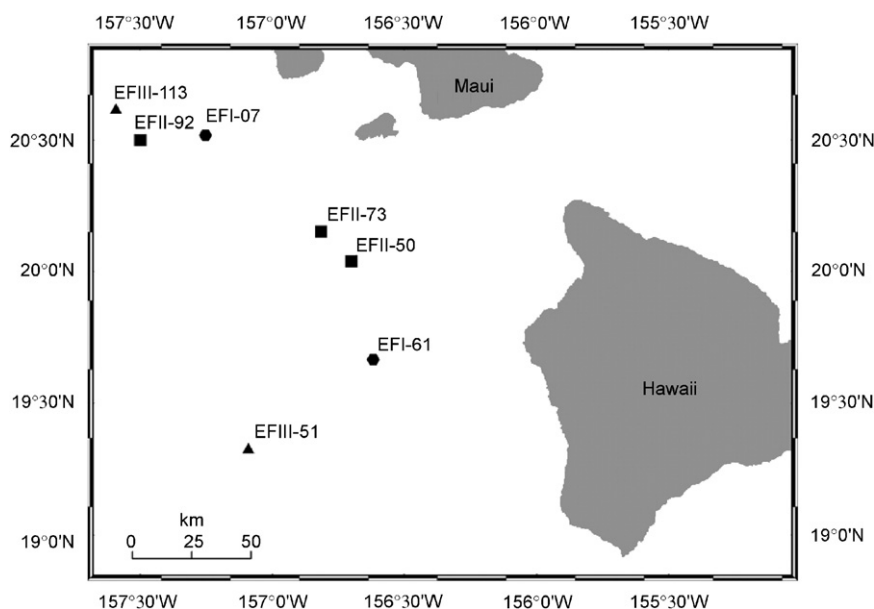


Fig. 1. Location of sampling casts during each E-Flux cruise. IN stations are EFlux I-61, EFlux II-50, EFlux II-73 and EFlux III-51. OUT stations are EFlux I-07, EFlux II-92 and EFlux III-113.

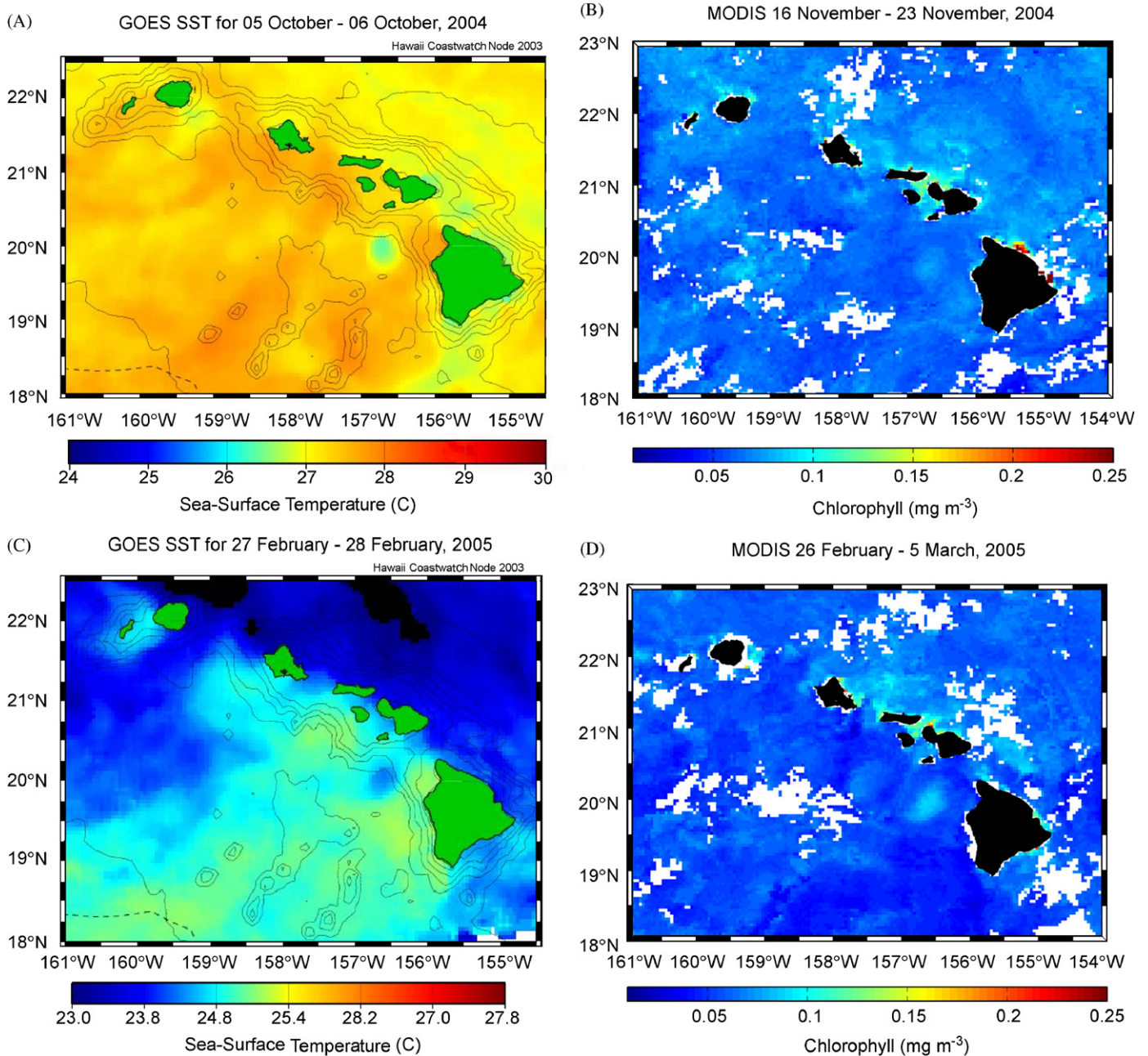


Fig. 2. Satellite GOES (Geostationary Operational Environmental Satellite) and MODIS (Moderate Resolution Imaging Spectroradiometer) images of the sampling area: (A) and (B) E-Flux I (Cyclone Noah); (C) and (D) E-Flux III (Cyclone Opal).

During each cruise, water-column samples were collected both within each eddy, IN stations, and in surrounding waters, or OUT stations (Table 1). The OUT stations were chosen for their distance from the eddy flow field, ambient background conditions, and relative proximity to the sampling area (Fig. 1). During E-Flux II, samples were collected from within the eddy generation region and include samples from one station within the centre of one of the two subsurface anomalies and a second set of samples from a station located between the two anomalies, where elevated total chlorophyll *a* (Chl *a*) concentrations were also observed.

2.2. Water-column ²¹⁰Po and ²¹⁰Pb

Discrete 10-L water-column samples for total ²¹⁰Po and ²¹⁰Pb analyses were collected using a CTD Rosette equipped with

Niskin-like bottles from 12 different depths over the upper 1000 m of the water column. The analytical methods followed those described in Nozaki (1986) and Masqué et al. (2002). Briefly, samples were immediately acidified, spiked with ²⁰⁹Po ($T_{1/2} = 102$ yr), and a stable Pb²⁺ yield tracer and Fe³⁺ carrier added. After 12 h of equilibration, the pH was adjusted to 8.5 with NH₄OH, and an Fe-precipitate (Fe(OH)₃) allowed to form and settle. The supernatant was carefully removed via siphoning and the precipitate transferred to 250-mL bottles. Radiochemical purification and measurement were conducted in the laboratory at Universitat Autònoma de Barcelona (UAB), to determine final ²¹⁰Pb and ²¹⁰Po activities. Once in the laboratory, the precipitate was dissolved in concentrated HCl and digested in an open vessel. Afterwards, the samples were diluted to 1 M HCl, the iron complexed with ascorbic acid, and Po plated onto silver discs. The remaining solution was replated in order to remove any

Table 1
Summary information of sampling dates and station locations

| Sampling cruise | IN stations | Latitude (°N), Longitude (°W) | OUT stations | Latitude (°N), Longitude (°W) |
|--------------------------------|---|----------------------------------|---------------------------|----------------------------------|
| E-Flux I (4–22 November 2004) | Cast 61 (14 November 2004) | 19.67, 156.62 | Cast 07 (5 November 2004) | 20.52, 157.25 |
| E-Flux II (10–28 January 2005) | Cast 50 (16 January 2005) | 20.04, 156.70 | Cast 92 (25 January 2005) | 20.50, 157.50 |
| E-Flux III (10–28 March 2005) | Cast 73 ^a (20 January 2005) Cast 51 (16 March 2005) | 20.15, 156.82 19.33, 157.09 | Cast 113 (24 March 2005) | 20.62, 157.59 |

^a Shear zone.

residual Po left in solution, which is typically less than 1%. The samples were counted on silicon surface-barrier alpha detectors long enough to achieve counting uncertainties of <5%. The plating solution was re-spiked with ²⁰⁹Po and stored for at least 6 months to allow for ²¹⁰Po ingrowth and to permit determination of ²¹⁰Pb by re-plating of the ²¹⁰Po. Pb yields were determined through measurement of stable Pb by atomic absorption spectrometry. Chemical recoveries of both ²¹⁰Po and ²¹⁰Pb ranged from 70% to 98%, averaging $80 \pm 10\%$. The ²¹⁰Po and ²¹⁰Pb activities were blank and decay-corrected to the date of collection.

2.3. Suspended and sinking particulate elemental analyses

Water column and sediment trap particulate carbon (PC), nitrogen (PN) and biogenic silica (bSiO₂) analyses are described in detail in Mahaffey et al. (2008) and Rii et al. (2008). Briefly, particle interceptor sediment traps (PITs) were pre-filled with a 1% formalin brine solution and were deployed at 150 m for a minimum of 3 days at both IN and OUT stations during E-Flux I and III. Trap material and 2-L water samples collected from discrete depths were filtered onto 25-mm combusted GF/F (PC and PN) or 0.8- μ m polycarbonate filters (bSiO₂). PC and PN filters were dried at 60 °C overnight, pelletized in tin foil cups, and concentrations determined using an elemental analyser (Carlo Erba NC2500) coupled to an isotope ratio mass spectrometer (ThermoFinnigan Delta S). Particulate bSiO₂ concentrations were determined using a weak NaOH digestion followed by a time-sensitive dilution technique with ammonium molybdate and a reducing agent (Paasche, 1980; Brzezinski and Nelson, 1995).

3. Results

3.1. Eddy flow fields

The physical and bio-optical properties of Cyclones *Noah* and *Opal* are discussed in detail in Kuwahara et al. (2008) and Nencioli et al. (2008). Both cyclones were characterized by significant uplift and biological response within the eddy core (Figs. 3 and 4). Satellite imagery suggests that Cyclone *Noah* was at least 2.5 months in age by the time of sampling, whereas Cyclone *Opal* was significantly younger, 4–5 weeks. Physically, Cyclone *Noah* was semi-elliptical in shape, and spanned ~ 100 km along its major axis based on the uplift of the 24.0 kg m^{-3} isopycnal surface ($\sigma_T = 24$). In contrast, Cyclone *Opal* was a substantially larger feature, spanning ~ 180 km and appeared much more circular and symmetric. While both had similar tangential velocities, uplift of the isopycnal surfaces in Cyclone *Noah* was limited to 50 m at the time of observation, whereas Cyclone *Opal*, had isopycnal displacements that were 2 times larger. These differences in isopycnal displacement and age likely led to the observed

differences in biomass and biological community structure (Landry et al., 2008; Rii et al., 2008).

Within Cyclone *Noah*, total Chl *a* mixed-layer concentrations increased by a factor of 1.3 relative to surrounding waters, mainly as a result of an increase in the 2–18 μ m nanoflagellates, such as pelagophytes and prymnesiophytes. A large, 3.6-fold increase in the >18- μ m size fraction was due to larger eukaryotes, such as pennate diatom species (Rii et al., 2008). Cyclone *Opal* had a similar ~ 1.5 fold increase in total Chl *a* within the eddy core, but there was a much greater ~ 7 -fold increase in the larger, >18- μ m size fraction due to the growth of diatoms (Rii et al., 2008). During E-Flux III, samples were also collected over a 10-day period within the eddy core in order to observe the evolution of the diatom bloom. During this time period, total Chl *a* concentrations decreased by 50%, and there was a transition from a diatom dominated community to smaller eukaryotes, pelagophytes and prymnesiophytes that were typical of Cyclone *Noah* and surrounding waters (Benitez-Nelson et al., 2007). The cause of the bloom decline is hypothesized to have been the result of silicic acid limitation (Benitez-Nelson et al., 2007; Rii et al., 2008). Combined, these results suggest that Cyclones *Noah* and *Opal* were in different biological stages of their evolution, with Cyclone *Noah* being within a decay phase, and Cyclone *Opal* in transition from mature to decay phase.

It is important to note here that Cyclones *Noah* and *Opal* were substantially different in their spatial movement after formation. While Cyclone *Noah* remained relatively stationary during sampling, and only slowly drifted to the South (Dickey et al., 2008), Cyclone *Opal* moved quite rapidly southward by ~ 165 km during E-Flux III (Nencioli et al., 2008). Nencioli et al. (2008) suggested that this rapid movement of Cyclone *Opal* resulted in an “open” or “leaky” bottom with the upper 75 m of Cyclone *Opal* acting as a closed system.

Samples collected from the eddy generation region in E-Flux II are considered to be representative of an eddy within the earliest stages of formation. Closer inspection of the eddy region shows two subsurface anomalies characterized by regions of minor isopycnal uplift spanning ~ 5 km and modest increases in total Chl *a* between the centre or shear zone of the two anomalies.

3.2. Water-column radionuclide profiles and flux results

²¹⁰Po and ²¹⁰Pb activities in the upper 200 m ranged from 7 to 17 dpm 100 L⁻¹ and from 14 to 35 dpm 100 L⁻¹, respectively (Fig. 5), and showed significant disequilibria (²¹⁰Po/²¹⁰Pb < 1) at all IN and OUT stations (Fig. 5). During E-Flux I, ²¹⁰Po/²¹⁰Pb profiles both within Cyclone *Noah* and surrounding waters were similar. At both stations, the highest depletion of ²¹⁰Po occurred between 100 and 150 m, just below the zone of maximum biomass. In E-Flux II the ²¹⁰Pb/²¹⁰Po profiles in the upper 75 m show similar patterns between the eddy generation region and the OUT station,

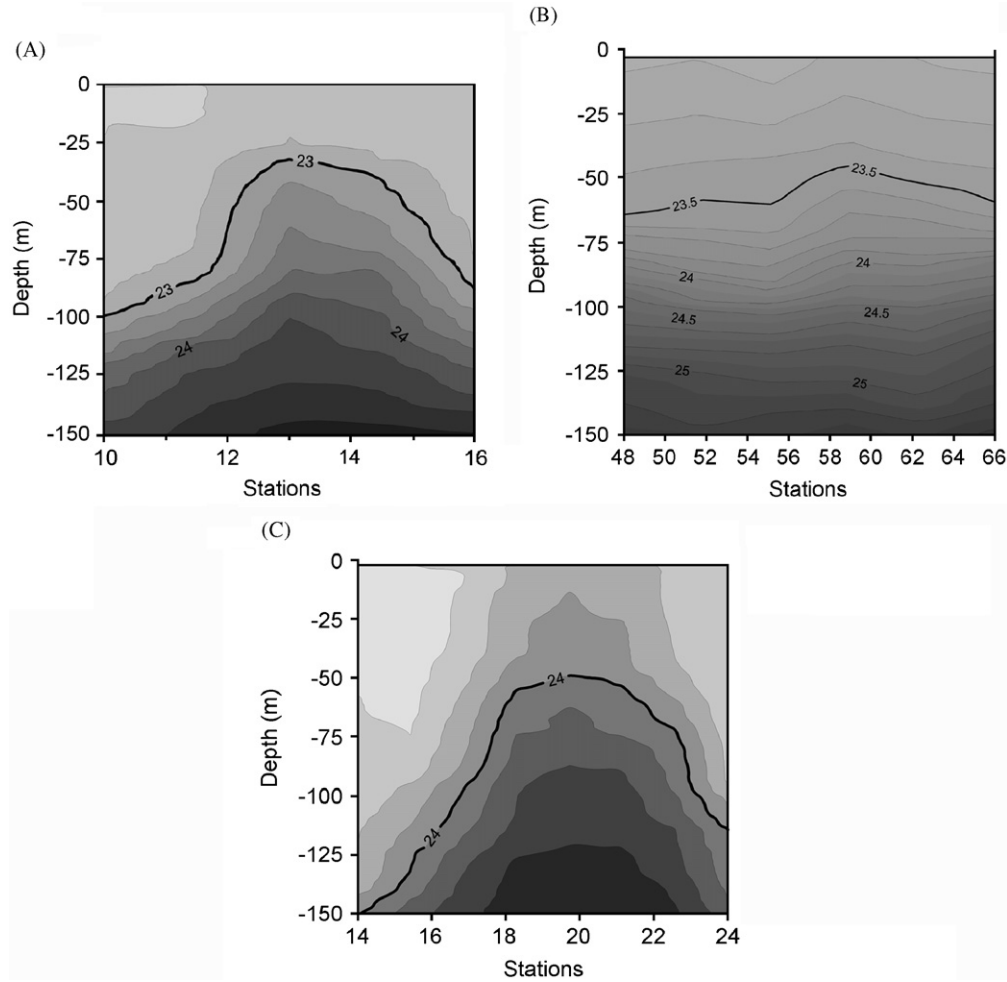


Fig. 3. Depth versus density profiles of the water column along a transect across (A) Cyclone *Noah* (E-Flux I), (B) eddy generation region (E-Flux II) and (C) Cyclone *Opal* (E-Flux III). The bold line represents σ_{23} , $\sigma_{23.5}$, and σ_{24} , respectively.

but with significantly larger (1.5–2-fold) disequilibria within the former. Below 75 m both profiles have the same trend, reflecting a large depletion of ^{210}Po centred at 150 m. Measurements within Cyclone *Opal* and surrounding waters showed large depletions in ^{210}Po over the upper 100 m. Below 100 m the disequilibrium is reduced at the IN station, whereas at the OUT station it is maintained throughout the water column.

The export flux of ^{210}Po can be estimated by solving the activity balance equation for total ^{210}Po :

$$\frac{\partial A_{\text{Po}}}{\partial t} = \Phi_{\text{Po}} + A_{\text{Pb}}\lambda_{\text{Po}} - A_{\text{Po}}\lambda_{\text{Po}} - P_{\text{Po}} + V \quad (1)$$

where Φ_{Po} is the input of atmospheric deposition of total ^{210}Po ($\text{dpm cm}^{-2} \text{d}^{-1}$), A_{Pb} and A_{Po} are the total ^{210}Pb and ^{210}Po measured activities ($\text{dpm } 100 \text{L}^{-1}$), λ_{Po} is the decay constant of ^{210}Po (0.00501d^{-1}), P_{Po} is the net removal flux of ^{210}Po ($\text{dpm m}^{-2} \text{d}^{-1}$), and V is the sum of advective and diffusive fluxes.

The removal flux may also be expressed in terms of the removal of ^{210}Po from the upper water column:

$$P_{\text{Po}} = A_{\text{Po}} \times k_{\text{Po}} \quad (2)$$

where k_{Po} is the scavenging rate constant (assumed to be first-order) for total Po removal from the water column (k_{Po} represents uptake and assimilation of Po onto particles and particle sinking). The inverse of k_{Po} represents the mean residence time of total ^{210}Po in the upper ocean (τ_{Po}).

Due to intense sampling and limited ship time, each station was only sampled once. As a result, steady state (SS, $\partial A_{\text{Po}}/\partial t = 0$) is assumed. We further ignore the atmospheric deposition of ^{210}Po (Φ_{Po}), as it is typically small, especially in open-ocean regions where it represents only $\sim 2\%$ of the *in situ* production of ^{210}Po from ^{210}Pb in the upper water column (Masqué et al., 2002). Kim et al. (2000) suggested that volatilization of ^{210}Po from the surface ocean may also occur, and suggested volatile ^{210}Po to be $\sim 0.1 \text{dpm } 100 \text{L}^{-1}$ in the coastal productive waters of Chesapeake Bay during windy conditions. This is significantly smaller than the observed inventories of ^{210}Po for the upper water column in our study and is ignored.

While advection and diffusion are often negligible in open-ocean systems, upwelling rates within cyclonic eddies, at least initially, are significant. In this case, upwelling would bring deep waters that are potentially richer in ^{210}Po to the surface, thereby masking ^{210}Po deficits due to particle scavenging. For example, assuming an upwelling velocity of 1m d^{-1} (Dickey et al., 2008) results in an underestimation of the particulate export from the euphotic zone by $\sim 15\%$. In this study, it appears that both Cyclones *Noah* and *Opal* experienced significant upwelling only during the initial stages of their formation and have remained closed systems, at least over the upper 75 m. Due to the lack of information regarding the eddy flow field within the eddy centre, all fluxes were determined assuming negligible physical processes and thus, should be considered minimum estimates.

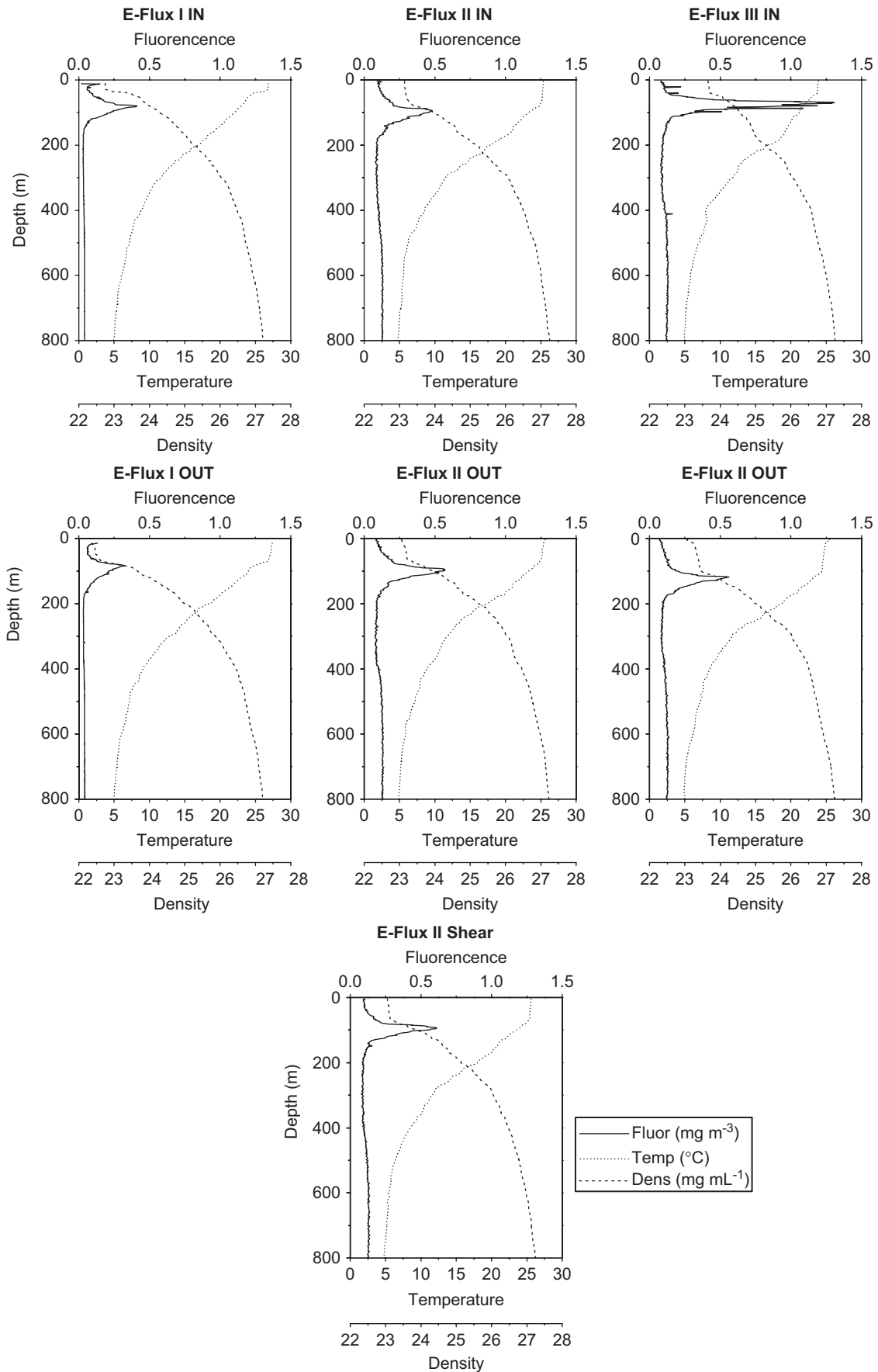


Fig. 4. Temperature, salinity and fluorescence (fluorometric chlorophyll) profiles for all stations examined in this study.

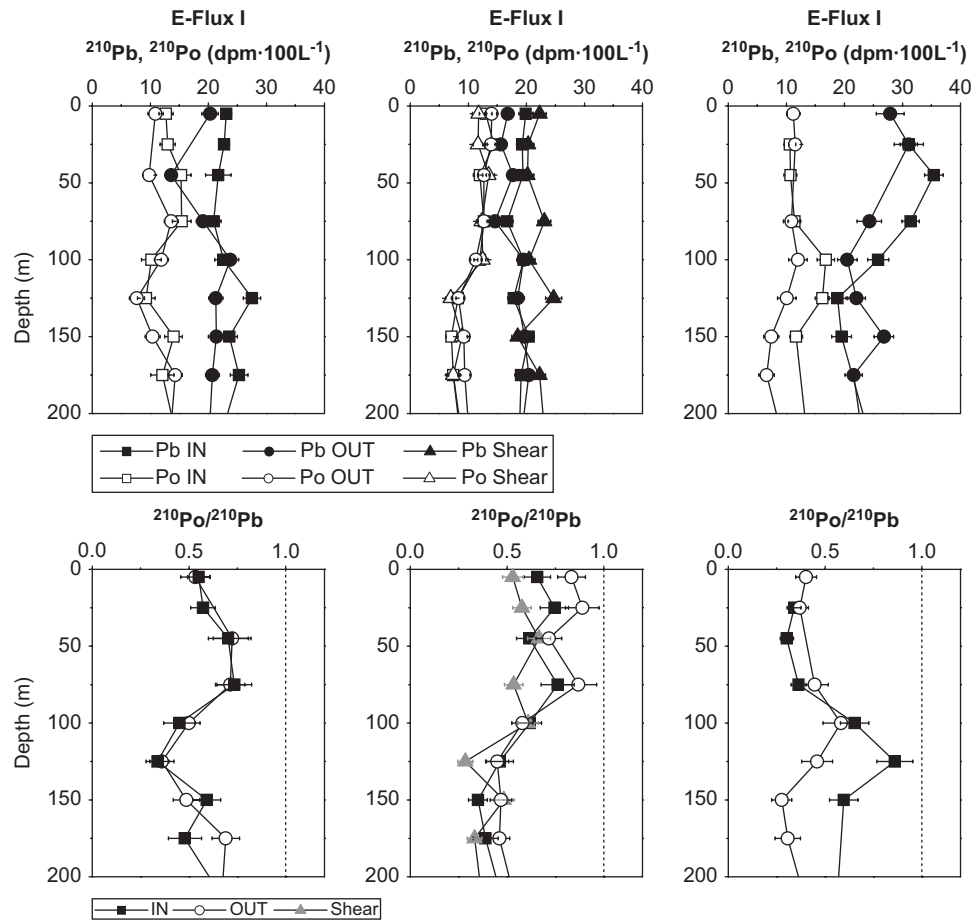


Fig. 5. Water-column profiles of ^{210}Pb and ^{210}Po total activities and the $^{210}\text{Po}/^{210}\text{Pb}$ activity ratio from 0 to 200 m.

Using these simplifications, the water-column flux of ^{210}Po can be calculated as

$$P_{\text{Po}} = \int (A_{\text{Pb}} - A_{\text{Po}}) \lambda_{\text{Po}} dz \quad (3)$$

where the integrated $^{210}\text{Po}/^{210}\text{Pb}$ disequilibrium was determined between 0–110 m and 0–150 m (Fig. 6). The 0–110 m section was chosen as it comprises the majority of the biomass as determined by total Chl *a* and microscopy, and lies just below the depth of the 1% light layer (Benitez-Nelson et al., 2007). The 0–150 m section was used to compare ^{210}Po -derived fluxes with eddy-induced fluxes obtained using PIT style sediment traps deployed at 150 m during each cruise (Rii et al., 2008) as well as with the standard trap depths used at both the Hawaii Ocean Time-series (HOT) and the Bermuda Atlantic Time-series stations (BATS).

Highest export of ^{210}Po occurred during the presence of Cyclone *Opal*, $113.8 \pm 6.1 \text{ dpm m}^{-2} \text{ d}^{-1}$ at 150 m. In contrast, within Cyclone *Noah* and the region of eddy formation, ^{210}Po fluxes were 30% and 50% lower, 77.7 ± 6.4 and $54.5 \pm 4.5 \text{ dpm m}^{-2} \text{ d}^{-1}$, respectively (Fig. 6, Table 2). The depth at which particle export occurred was also substantially different. Within Cyclone *Noah* and the eddy formation region, particle export almost doubled with increasing integration depth from 110 to 150 m, whereas the majority of Cyclone *Opal*'s export was constrained to the upper 110 m (Table 2). In comparison, the magnitude of ^{210}Po export varied significantly at the OUT stations, with the highest export also occurring during E-Flux III, $110.1 \pm 8.3 \text{ dpm m}^{-2} \text{ d}^{-1}$ at 150 m. The ^{210}Po flux was almost 2 to 3-fold smaller during E-Flux I and E-Flux II, 64.9 ± 5.4 and $42.4 \pm 4.2 \text{ dpm m}^{-2} \text{ d}^{-1}$, respectively.

3.3. ^{210}Po derived PC, PN and $b\text{SiO}_2$ fluxes

Estimating particulate carbon (PC) export requires knowledge of not only the ^{210}Po flux, but the $\text{PC}/^{210}\text{Po}$ ratio in sinking particles across the depth horizon of interest. Unfortunately, this ratio was not determined in this study due to the decay of ^{210}Po within the particulate samples. Therefore, we used a range of $\text{PC}/^{210}\text{Po}$ ratios measured in sediment trap material at the base of the euphotic zone (100–200 m) in other studies (Table 3). Please note that $\text{PN}/^{210}\text{Po}$ ratios were not published in these papers. Murray et al. (2005) measured $\text{PC}/^{210}\text{Po}$ ratios in the equatorial Pacific, ranging from 102 to $358 \mu\text{mol C dpm}^{-1}$, and averaged $202 \pm 89 \mu\text{mol C dpm}^{-1}$ ($n = 9$). Using this average ratio and our ^{210}Po export rates, we estimate PC fluxes of 8 – $21 \text{ mmol C m}^{-2} \text{ d}^{-1}$ at 110 m, and 13 – $23 \text{ mmol C m}^{-2} \text{ d}^{-1}$ at 150 m. In the north-western Mediterranean, Stewart et al. (2007a) found a similar range in $\text{PC}/^{210}\text{Po}$ ratios (66 – $309 \mu\text{mol C dpm}^{-1}$, $n = 11$), but with a weighted average value a factor of two lower, $102 \pm 1 \mu\text{mol C dpm}^{-1}$. Using Stewart et al.'s average ratio, we obtain PC fluxes ranging from 5 to $11 \text{ mmol C m}^{-2} \text{ d}^{-1}$ at 110 m, and from 7 to $11 \text{ mmol C m}^{-2} \text{ d}^{-1}$ at 150 m. In a similar study of eddies in the Sargasso Sea, Buesseler et al. (2008) found an even lower range in the $\text{PC}/^{210}\text{Po}$ ratio, 25 to $58 \mu\text{mol C dpm}^{-1}$ ($n = 4$), with an average ratio of $43 \pm 9 \mu\text{mol C dpm}^{-1}$. Using this value, we obtain significantly lower carbon export rates, of about 2 – $4 \text{ mmol C m}^{-2} \text{ d}^{-1}$ at 110 m, and 3 – $5 \text{ mmol C m}^{-2} \text{ d}^{-1}$ at 150 m. The wide ranges in $\text{PC}/^{210}\text{Po}$ ratios reported from these studies are likely due to a mixture of processes related to particle formation (i.e. biological community structure, degradation rate, particle size, etc.).

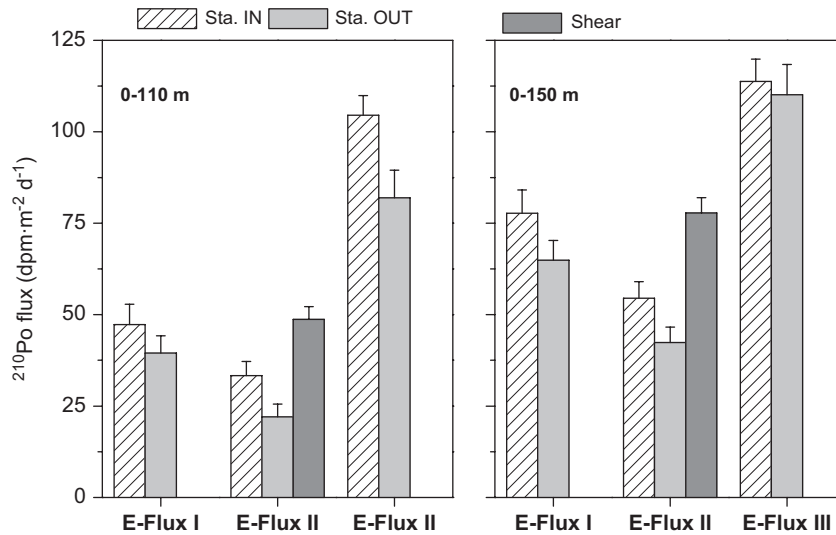


Fig. 6. ^{210}Po fluxes integrated over the 0–110 m and 0–150 m at each station.

Table 2
 ^{210}Po fluxes integrated over the upper 0–110 and 0–150 m depth intervals

| Cruise | Depth (m) | ^{210}Po Flux (P) ($\text{dpm m}^{-2} \text{d}^{-1}$) | | |
|------------|-----------|--|-----------------|----------------|
| | | IN | OUT | Shear |
| E-Flux I | 110 | 47.3 ± 5.5 | 39.5 ± 4.7 | |
| C. Noah | 150 | 77.7 ± 6.4 | 64.9 ± 5.4 | |
| E-Flux II | 110 | 33.3 ± 3.9 | 22.0 ± 3.5 | 48.7 ± 3.5 |
| C. Victor | 150 | 54.5 ± 4.5 | 42.4 ± 4.2 | 77.8 ± 4.2 |
| E-Flux III | 110 | 104.5 ± 5.4 | 81.9 ± 7.6 | |
| C. Opal | 150 | 113.8 ± 6.1 | 110.1 ± 8.3 | |

PC fluxes were also estimated using suspended water-column PC measurements and the residence times of ^{210}Po over the depth interval of interest (i.e. 0–110 m or 0–150 m, see Table 4). The residence time of ^{210}Po (τ_{Po}) is given by the inverse of k_{Po} , the scavenging rate constant, as described in Eq. (2). The PC export flux is therefore obtained using Eq. (5) (Shimmield et al., 1995):

$$\text{PC flux} = \frac{I(\text{PC})}{\tau_{\text{Po}}} \quad (5)$$

where $I(\text{PC})$ is the inventory of PC in the water column calculated using the bottle derived particle measurements discussed above. This approach assumes that ^{210}Po and organic matter (e.g., PC) have the similar residence times in the water column, and that the deficit in ^{210}Po relative to ^{210}Pb is due to sinking organic matter. Previous evidence, although limited, suggests that this is indeed the case, with laboratory experiments showing that ^{210}Po 's distribution inside plankton is similar to that of protein, and that ^{210}Po is lost from decomposing marine particles at the same rate as organic C. This follows a number of other field studies showing that ^{210}Po is enriched in organic tissue and correlates well with PC (Fowler and Knauer, 1986; Cherry and Heyraud, 1988; Fisher et al., 1983; Friedrich and Rutgers van der Loeff, 2002; Stewart and Fisher, 2003a,b; Stewart et al., 2005, 2007a; Murray et al., 2005). We should note here that we are using particulate samples collected using Niskin bottles and that these samples likely contain suspended material as well. There is quite a bit of literature on the collection of sinking and suspended particles using sediment traps and bottles, and we argue that neither

collection method is perfect (e.g., Gardner et al., 2003; Liu et al., 2005). For example, *in situ* pumps may result in particle formation and/or break-up, whereas Niskins may miss those rare large sinking particles. Conversely, it has been shown that Niskins may better collect motile zooplankton (Liu et al., 2005). If suspended matter does dominate the particles collected here, it is possible that we would overestimate the residence time of PC and our flux estimates would be too low.

The PC, PN, and bSiO_2 fluxes at 150 m were estimated using Eq. (5) (Tables 4 and 5). For E-Flux I (Cyclone Noah) the PC fluxes were calculated to be $1.71 \pm 0.16 \text{ mmol C m}^{-2} \text{d}^{-1}$ within the eddy core, relative to $1.69 \pm 0.16 \text{ mmol C m}^{-2} \text{d}^{-1}$ at the OUT stations. For E-Flux III (Cyclone Opal) the PC flux results are $1.58 \pm 0.10 \text{ mmol C m}^{-2} \text{d}^{-1}$ inside the eddy, and $1.67 \pm 0.16 \text{ mmol C m}^{-2} \text{d}^{-1}$ at the OUT stations. For E-Flux II, the PC fluxes could not be determined due to the lack of elemental data for the corresponding stations. The PN fluxes at 150 m for E-Flux I (Cyclone Noah) are $0.22 \pm 0.02 \text{ mmol N m}^{-2} \text{d}^{-1}$ within the eddy core, relative to $0.26 \pm 0.03 \text{ mmol N m}^{-2} \text{d}^{-1}$ at the OUT stations. For E-Flux III (Cyclone Opal) the PC flux results are $0.30 \pm 0.02 \text{ mmol N m}^{-2} \text{d}^{-1}$ inside the eddy, and the same magnitude, $0.30 \pm 0.03 \text{ mmol N m}^{-2} \text{d}^{-1}$, at the OUT stations. Within Cyclone Opal (the only cruise from which bSiO_2 data are available), bSiO_2 fluxes were $0.157 \pm 0.010 \text{ mmol Si m}^{-2} \text{d}^{-1}$ relative to $0.025 \pm 0.002 \text{ mmol Si m}^{-2} \text{d}^{-1}$ at the OUT stations, i.e. more than 6 times higher at the IN stations versus surrounding waters.

4. Discussion

The open ocean is typically characterized by nutrient- and trace-metal-limited regenerated production. New production results only when external nutrients, such as upwelling from below or atmospheric deposition from above, enters the system. At steady state, these new nutrients are hypothesized to result in the flux of particles from surface to depth. Several studies have suggested that the upwelling of nutrient-rich deep waters into the surface via mesoscale eddies may significantly add to primary production and carbon export in the open ocean (Falkowski et al., 1991; Allen et al., 1996; McGillicuddy et al., 1998; Siegel et al., 1999). The magnitude of this new production and export, however, strongly depends on the evolution of the biological community.

Table 3

PC fluxes from the upper 0–110 and 0–150 m, derived from ^{210}Po using the $\text{PC}/^{210}\text{Po}$ ratio from other studies measured in sediment trap material at the base of the euphotic zone (100–200 m)

| Reference work and area | Range of $\text{PC}/^{210}\text{Po}$ ($\mu\text{mol C dpm}^{-1}$) | Average $\text{PC}/^{210}\text{Po}$ ($\mu\text{mol C dpm}^{-1}$) | PC Flux ^a at 110 m ($\text{mmol C m}^{-2} \text{d}^{-1}$) | PC Flux ^a at 150 m ($\text{mmol C m}^{-2} \text{d}^{-1}$) |
|--|--|---|---|---|
| Murray et al. (2005), Equatorial Pacific | 102–358 ($n = 9$) | 202 ± 89 | 8–21 | 13–23 |
| Stewart et al. (2005), NW Mediterranean | 66–309 ($n = 11$) | 102 ± 1 | 5–11 | 7–11 |
| Buesseler et al. (2008), Sargasso Sea | 25–58 ($n = 4$) | 43 ± 9 | 2–4 | 3–5 |

^a PC fluxes calculated using the average $\text{PC}/^{210}\text{Po}$ ratio.

Table 4

Residence times of ^{210}Po and inventories of PC, PN and bSiO_2 in the upper 0–110 and 0–150 m of the water column

| Cruise | Depth (m) | ^{210}Po residence time (d) | | Inventory PC (mmol C m^{-2}) | | Inventory PN (mmol N m^{-2}) | | Inventory bSiO_2 ($\mu\text{mol Si m}^{-2}$) | |
|------------|-----------|--------------------------------------|--------------|---|-----|---|-----|---|-----|
| | | IN | OUT | IN | OUT | IN | OUT | IN | OUT |
| E-Flux I | 110 | 314 ± 40 | 118 ± 42 | 341 | 331 | 44 | 52 | | |
| C. Noah | 150 | 247 ± 23 | 248 ± 24 | 423 | 418 | 54 | 65 | | |
| E-Flux III | 110 | 111 ± 8 | 138 ± 15 | 247 | 181 | 44 | 33 | 25 | 1.4 |
| C. Opal | 150 | 169 ± 11 | 147 ± 14 | 266 | 246 | 51 | 44 | 27 | 3.6 |

Table 5

PC, PN and bSiO_2 fluxes derived from ^{210}Po using the water column inventory of PC, PN and bSiO_2 integrated over the upper 0–110 and 0–150 m

| Cruise | Depth (m) | IN | | OUT | | IN | | OUT | |
|------------|-----------|--|-------------------|---|--|--|--|---|--|
| | | PC Flux ($\text{mmol C m}^{-2} \text{d}^{-1}$) | | PC Trap Flux ($\text{mmol C m}^{-2} \text{d}^{-1}$) | | PN Flux ($\text{mmol C m}^{-2} \text{d}^{-1}$) | | PN Trap Flux ($\text{mmol C m}^{-2} \text{d}^{-1}$) | |
| E-Flux I | 110 | 1.09 ± 0.14 | 1.04 ± 0.14 | | | | | | |
| C. Noah | 150 | 1.71 ± 0.16 | 1.69 ± 0.16 | | | 2.20 ± 0.23 | | 2.31 ± 0.26 | |
| E-Flux III | 110 | 2.22 ± 0.16 | 1.32 ± 0.15 | | | | | | |
| C. Opal | 150 | 1.58 ± 0.10 | 1.67 ± 0.16 | | | 1.55 ± 0.11 | | 1.52 ± 0.20 | |
| E-Flux I | 110 | 0.14 ± 0.02 | 0.16 ± 0.02 | | | | | | |
| C. Noah | 150 | 0.22 ± 0.02 | 0.26 ± 0.03 | | | 0.40 ± 0.03 | | 0.43 ± 0.05 | |
| E-Flux III | 110 | 0.40 ± 0.03 | 0.24 ± 0.03 | | | | | | |
| C. Opal | 150 | 0.30 ± 0.02 | 0.30 ± 0.03 | | | 0.25 ± 0.02 | | 0.28 ± 0.04 | |
| E-Flux III | 150 | 0.157 ± 0.010 | 0.025 ± 0.002 | | | | | | |
| C. Opal | 150 | | | | | 0.427 ± 0.034 | | 0.111 ± 0.065 | |

Trap fluxes were obtained from sediment trap (PIT design) deployed at 150 m (from Rii et al., 2008).

Mesoscale eddies that form in the lee of the main Hawaiian Islands provide an ideal laboratory for attempting to understand eddy driven processes. Both island topography and the prevailing north-easterly trade winds combine to generate a vigorous and continuous eddy field in the lee of the Island of Hawaii, such that eddies, on the order of 100 km in diameter, are formed throughout the year during periods of intense trade wind activity (October–March) (Patzert, 1969; Lumpkin, 1998). The E-Flux program provided a unique opportunity to study the particle export that resulted from two mesoscale eddies of different ages and biological community structure: cyclones *Noah* and *Opal*. Biological and physical measurements suggest that Cyclone *Opal* was a large well-developed eddy towards the end of its biological maturity as characterized by the observed cessation of a diatom bloom, likely due to silicic acid limitation (Benitez-Nelson et al., 2007; Rii et al., 2008). Cyclone *Noah* was older and less well formed, with a biological community well into its decay phase as evidenced by smaller eukaryotes and low nutrient levels. Sweeney et al. (2003) proposed an age-based model of the lifetime of a

mesoscale eddy. According to this model, one would expect significant export from both cyclones *Noah* and *Opal*, with Cyclone *Opal* in the midst of a large export event due to the crash of the diatom bloom, and Cyclone *Noah* depicting remnants of an export event that occurred within the preceding months.

In contrast to ^{234}Th – ^{238}U disequilibria and short-term sediment-trap-derived export, ^{210}Pb – ^{210}Po disequilibria tracks particle formation and sinking on timescales of months to a year. As such, this radionuclide pair is well suited for following particle export from a mesoscale eddy whose biological community is well into its decay phase. In addition, ^{210}Po has a characteristic biogeochemistry in seawater, in that, unlike ^{234}Th , its partitioning within the cell is similar to that of proteins and sulphur, being assimilated in the cytoplasm of some species of phytoplankton (Stewart and Fisher, 2003a,b; Stewart et al., 2005, 2007). Therefore, ^{234}Th is adsorbed in the surface, whereas ^{210}Po is incorporated into the cell, just like carbon and other nutrients.

Measurements of ^{210}Po export showed a progressive cycle in the absolute magnitude of particle export, starting with relatively

low particle export within the eddy generation region (E-Flux II), to an almost doubling of export within Cyclone *Opal*, before decreasing again to moderately low levels within Cyclone *Noah*. Higher export rates within the “shear” zone between the two anomalies encountered in the eddy formation region during E-Flux II, suggest that this may have been a zone of enhanced nutrient availability, and thus primary production and export (Table 2, Fig. 6).

The ^{210}Po flux determined within each eddy provides an estimate of the absolute magnitude of particle export and hence the potential capacity of each eddy to transport fixed carbon to depth. However, cyclones *Noah* and *Opal* were sampled during different seasons, and, indeed, this is evidenced by the large changes in particle export observed at the OUT stations. Given the longer residence time of ^{210}Po in the water column, it is expected to record seasonal changes in particle flux that are not captured by short-term sediment trap deployments or short-lived radionuclides, such as ^{234}Th . Thus, direct comparisons between eddies may be misleading. We therefore propose a second mechanism to evaluate the relative strength of each eddy: by normalizing to the OUT station sampled during that same cruise. This practice allows one to consider seasonal processes that may not otherwise be identified by the comparison of absolute ^{210}Po fluxes as above, and enables a more detailed analysis of the relative strength of each eddy. In this manner, we hope to minimize the fact that the eddies were not sampled synoptically.

The results from the normalization process are shown in Fig. 7. For the 0–110 m depth interval, the export flux of ^{210}Po is ~20% higher at IN versus OUT stations for E-Flux I (*Noah*), ~30% higher for E-Flux III (*Opal*), and ~50% to 120% higher for E-Flux II (in this last instance depending on whether the station was within an anomaly or between the anomalies coincident with elevated total Chl *a* concentrations). For the 0–150 m depth interval, differences were less dramatic, with ^{210}Po fluxes only 20% higher within Cyclone *Noah* and the same, within error, at the core of Cyclone *Opal* relative to surrounding waters. Particle fluxes at 150 m within the eddy generation region (E-Flux II) were 30% and 80% higher. Therefore, using this analysis, particle export within cyclones *Noah* and *Opal* were at most, only modestly enhanced. Only the “shear” station within the eddy generation region had particle export rates that significantly exceeded that determined at the OUT stations.

We should note here that the OUT stations were chosen so as to be outside the zone of eddy influence but as close to the sampling site as possible. As a result, these stations were generally

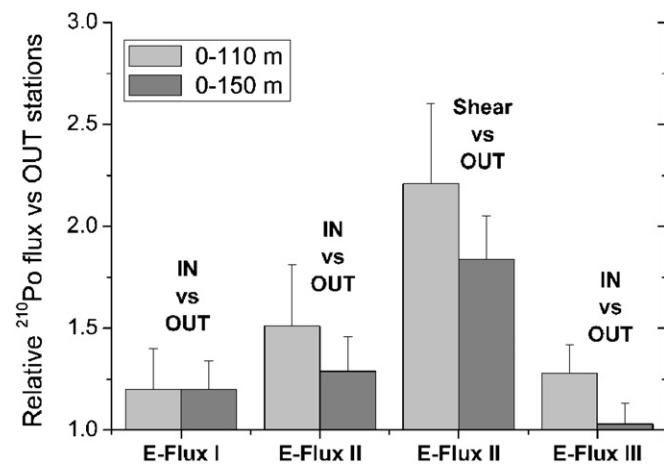


Fig. 7. Relative ^{210}Po export fluxes for IN (and shear) stations versus OUT stations.

taken closer to land. It is possible that seasonal processes at these OUT stations are not representative of processes further offshore, particularly over the longer integration periods of ^{210}Pb – ^{210}Po disequilibrium. For example, the high disequilibrium at the OUT stations during E-Flux I and III may be due to remnants of coastal blooms or terrigenous material that had been advected offshore, although no direct evidence of either phenomena were observed.

Closer examination of water-column ^{210}Pb – ^{210}Po disequilibrium shows that most of the particle export occurs within the upper 150 m of Cyclone *Noah*, whereas for Cyclone *Opal* export was mostly constrained to the upper 110 m. This is consistent with the observed biological community structure, biomass and growth and grazing estimates (Landry et al., 2008; Rii et al., 2008), and higher primary production rates within this feature. The deficiency of ^{210}Po decreased significantly from 110 to 150 m for Cyclone *Opal*, suggesting rapid remineralization of particles within this depth interval. Similar signatures of rapid remineralization have been observed in ^{238}U – ^{234}Th disequilibria within Cyclone *Opal* (Maiti et al., 2008) consistent with a decrease in dissolved O_2 concentrations between 90 and 130 m (Nencioli et al., 2008).

The PC export rates derived using the PC/ ^{210}Po ratios of Murray et al. (2005) and Stewart et al. (2007a) are considerably higher than the average $1.8 \pm 0.9 \text{ mmol C m}^{-2} \text{ d}^{-1}$ measured at 150 m within Cyclone *Opal* using sediment traps ($1.54 \pm 0.11 \text{ mmol C m}^{-2} \text{ d}^{-1}$), ^{234}Th ($0.97 \pm 0.57 \text{ mmol C m}^{-2} \text{ d}^{-1}$), and ^{15}N mass balance ($2.8 \pm 0.8 \text{ mmol C m}^{-2} \text{ d}^{-1}$) (Benitez-Nelson et al., 2007). The sediment trap flux at 150 m recorded during E-Flux I within Cyclone *Noah* was $2.20 \pm 0.23 \text{ mmol C m}^{-2} \text{ d}^{-1}$ and similar to that measured during E-Flux II within the eddy generation region of $1.91 \pm 0.12 \text{ mmol C m}^{-2} \text{ d}^{-1}$ (Rii et al., 2008). Only the PC fluxes derived using the Buesseler et al. (2008) PC/ ^{210}Po ratio from eddies encountered in the Sargasso Sea give PC fluxes that are similar to the other independent determinations of particle flux in the E-Flux program. This is not surprising given that both studies sampled eddies that had biological communities which appeared to be dominated by diatoms.

Using the residence time of ^{210}Po and the inventory of PC in the water column (residence time model), PC fluxes were calculated for both cyclones *Noah* and *Opal* and at the OUT stations. During E-Flux III, PC fluxes integrated over the upper 0–150 m were $1.58 \pm 0.10 \text{ mmol C m}^{-2} \text{ d}^{-1}$ within Cyclone *Opal*, and $1.67 \pm 0.16 \text{ mmol C m}^{-2} \text{ d}^{-1}$ at the OUT station. These fluxes are consistent with Cyclone *Opal* particle export rates ranging from a low of $0.97 \pm 0.57 \text{ mmol C m}^{-2} \text{ d}^{-1}$ using ^{234}Th to a maximum of 2.8 ± 0.8 using ^{15}N mass balance (Benitez-Nelson et al., 2007; Maiti et al., 2008). For E-Flux I, the ^{210}Po -derived PC export over the upper 150 m was $1.71 \pm 0.16 \text{ mmol C m}^{-2} \text{ d}^{-1}$ within Cyclone *Noah* and $1.69 \pm 0.16 \text{ mmol C m}^{-2} \text{ d}^{-1}$ in surrounding waters, only slightly lower than the $2.20 \pm 0.23 \text{ mmol C m}^{-2} \text{ d}^{-1}$ determined using sediment traps (Rii et al., 2008). None of these other estimates found significant differences in PC export between the Cyclones and the OUT stations. While it is possible that the majority of particle export had yet to occur in Cyclone *Opal*, this would not have been the case for Cyclone *Noah*.

The PN fluxes derived from ^{210}Po during E-Flux I were about 40% lower than those recorded in sediment traps, both within the eddy and at the OUT station. Conversely, for E-Flux III ^{210}Po derived PN fluxes were larger by about 10–20% than the sediment trap fluxes.

In contrast to PC and PN, the flux of bSiO_2 within Cyclone *Opal* was more than 6 times larger than that found in surrounding waters ($0.157 \pm 0.010 \text{ mmol Si m}^{-2} \text{ d}^{-1}$ relative to $0.025 \pm 0.002 \text{ mmol Si m}^{-2} \text{ d}^{-1}$). These absolute fluxes are considerably lower than those measured in sediment traps ($0.427 \pm 0.034 \text{ mmol Si m}^{-2} \text{ d}^{-1}$ inside *Opal*, and $0.111 \pm 0.065 \text{ mmol Si m}^{-2} \text{ d}^{-1}$

outside the eddy) (Benitez-Nelson et al., 2007), but similar, or slightly higher, to those estimated using ^{234}Th , 0.145 ± 0.110 and $0.100 \pm 0.027 \text{ mmol Si m}^{-2} \text{ d}^{-1}$ at the IN and OUT stations, respectively (Maiti et al., 2008). It is interesting to note that the difference in bSiO_2 fluxes between IN and OUT stations derived from ^{210}Po is substantially greater than the factor of 2–4 difference determined using the other techniques. These low bSiO_2 fluxes observed at the OUT stations support the hypothesis that Hawaiian eddies are much more efficient in exporting silica relative to PC, PN and other elements (Benitez-Nelson et al., 2007; Landry et al., 2008; Rii et al., 2008).

Primary production (PP) measured inside Cyclone *Opal* based on phytoplankton growth estimates was $128 \pm 16 \text{ mmol C m}^{-2} \text{ d}^{-1}$, and the gross primary production (GPP) determined from $\Delta^{17}\text{O}$ was very similar, $125 \pm 6 \text{ mmol C m}^{-2} \text{ d}^{-1}$ (Benitez-Nelson et al., 2007). Thus, the calculated f -ratio (PC export to total PP) is <0.012 , comparable to that measured at Station ALOHA and typical of export ratios measured in other open-ocean systems. Therefore, Cyclone *Opal* was surprisingly inefficient in transporting PC to depth, which is consistent with the other export measurements determined in this study (Benitez-Nelson et al., 2007; Maiti et al., 2008; Rii et al., 2008). ^{210}Po -derived and sediment trap results from the older, later stage eddy, Cyclone *Noah*, also showed little to no enhanced carbon export relative to surrounding waters.

High bSiO_2 and low PC fluxes within Cyclone *Opal* were further confirmed by microscopic images of generally empty but intact diatom frustules within the sediment trap material (Benitez-Nelson et al., 2007; Rii et al., 2008). These results support Ingalls et al. (2006), who suggested that organic matter in diatom rich regions are more heavily processed by zooplankton, and hypothesized that diatoms can potentially export a higher proportion of silica as highly silicified empty frustules that contain relatively less but unaltered organic matter. This is also in agreement with what we know about the organic matter load carrying capacity of different ballast types, as it is suggested that in general calcium carbonate appears to carry the largest loading of organic matter while silica carries the smallest (Klaas and Archer, 2002).

As a result, despite a substantial 3-fold enhancement in primary production (Benitez-Nelson et al., 2007), remineralization played an important role within both eddy systems. Recycling was probably greatly facilitated by strong microzooplankton grazing relative to macrozooplankton grazing (Landry et al., 2008), and a shift in bacterial community composition. Combined, these processes led to a more intense and shallower zone of remineralization than that observed in the surrounding waters, including Station ALOHA, such that eddy particle fluxes are similar to the average PC fluxes measured at the time-series site, $2.4 \pm 0.6 \text{ mmol C m}^{-2} \text{ d}^{-1}$ (Karl et al., 1996; Benitez-Nelson et al., 2001; Maiti et al., 2008). Within Cyclone *Opal*, mass balance estimates of organic C production and export suggest that more than 85% of net community production accumulated in the upper 110 m in the dissolved phase rather than being exported as PC (Benitez-Nelson et al., 2007).

These results suggest that cyclonic eddies formed in subtropical waters may not necessarily be an effective mechanism for exporting PC to the mesopelagic zone. This finding is consistent with a recent temperature-dependent food web model that predicts low carbon export efficiencies on waters with surface temperatures exceeding 25°C (Laws et al., 2000; Benitez-Nelson et al., 2007). Our results confirm that wind-driven eddies can be highly productive and can increase biomass, but they are not necessarily more efficient in exporting PC to deeper waters. Rather, they appear to be more effective as a silica pump. This finding is similar to that found within mature eddies in the Sargasso Sea (Buesseler et al., 2008). However, a retrospective analysis of thorium-based export fluxes at the BATS time-series

did suggest increased export in younger eddies (Sweeney et al., 2003).

5. Conclusions

The $^{210}\text{Po}/^{210}\text{Pb}$ profiles suggest that, for all cases, export fluxes are at most, only moderately enhanced within cyclonic eddies in the lee of the Hawaiian Islands relative to surrounding waters (Fig. 6, Table 2). This result of low export recorded within the eddies was in principle unexpected, given that primary production, at least within Cyclone *Opal*, was high and the plankton community composed of larger, presumably faster sinking organisms, such as diatoms. Rather, the particulate flux within the upper 110 m, appears to have been rapidly remineralized by 150 m depth. A similar signature of remineralization was observed by the ^{238}U – ^{234}Th disequilibria (Maiti et al., 2008). Strong microzooplankton grazing and bacterial remineralization are the likely cause for the reduced PC and PN export and the highly inefficient fluxes that occurred within these mesoscale features. This fact is consistent with recent models of the pelagic food web that account for the role of temperature on export production. Laws et al. (2000) suggest that f -ratios are low at all rates of production at temperature $\geq 25^\circ\text{C}$, such as the warm waters of the subtropical North Pacific Gyre. It is interesting to note that within Cyclone *Opal*, the export flux was dominated by empty diatom frustules, suggesting the possibility that Hawaiian lee eddies are “silica pumps”. This exciting result requires more detailed future studies of silica uptake and export within mesoscale features.

Measuring what controls the magnitude, timing, and depth of surface water particle export in marine systems is a difficult task and the focus of a multitude of current research programs (e.g., Boyd and Trull, 2007). Similarities in the ^{210}Po -derived export fluxes of PC, PN, and bSiO_2 to other independent tracers used within the E-Flux program, i.e. sediment traps, ^{234}Th , and ^{15}N mass balance, provides confidence in our approach. It further suggests that the residence time model used here provides another independent means of estimating particle flux in the ocean, despite all of the inherent assumptions in the PC/ ^{210}Po ratio and the inventories of PC, PN and bSiO_2 determined using Niskin bottles. Thus, these results suggest that the application and use of ^{210}Pb – ^{210}Po disequilibria as a tracer of particle export should be investigated more fully.

Acknowledgements

We thank Carrie Leonard and the NOAA Coastwatch Pacific Node (Honolulu Hawaii) for the GOES and MODIS satellite imagery, Victor Kuwahara, Francesco Nencioli and Tommy Dickey for the CTD data, and Yoshimi Rii for supplying the suspended bSiO_2 data. The E-Flux program was funded by the Ocean Sciences Division of the National Science Foundation and EV supported by a Ph.D. fellowship from the Ministerio de Educación y Ciencia of Spain.

References

- Allen, C.B., Kanda, J., Laws, E.A., 1996. New production and photosynthetic rates within and outside a cyclonic mesoscale eddy in the North Pacific subtropical gyre. *Deep-Sea Research I* 43, 917–936.
- Benitez-Nelson, C., Buesseler, K.O., Karl, D.M., Andrews, J.E., 2001. A time-series study of particulate matter export in the North Pacific Subtropical Gyre based on ^{234}Th – ^{238}U disequilibrium. *Deep-Sea Research I* 48, 2595–2611.
- Benitez-Nelson, C., Bidigare, R.R., Dickey, T.D., Landry, M.R., Leonard, C.L., Brown, S.L., Nencioli, F., Rii, Y.M., Maiti, K., Becker, J.W., Bibby, T.S., Black, W., Cai, W.J., Carlson, C., Chen, F.Z., Kuwahara, V.S., Mahaffey, C., McAndrew, P.M., Quay, P.D., Rappé, M., Selph, K.E., Simmons, M.E., Yang, E.J., 2007. Eddy induced diatom

- bloom drives increased biogenic silica flux, but inefficient carbon export in the subtropical North Pacific Ocean. *Science* 312, 1017–1021.
- Boyd, P.W., Trull, T.W., 2007. Understanding the export of biogenic particles in oceanic waters: is there consensus? *Progress in Oceanography* 72, 276–312.
- Brzezinski, M.A., Nelson, D.M., 1995. The annual silica cycle in the Sargasso Sea near Bermuda. *Deep-Sea Research I* 42, 1215–1237.
- Buesseler, K.O., Lamborg, C., Cai, P., Escoube, R., Johnson, R., Pike, S., Masqué, P., McGillicuddy, D., Verdeny, E., 2007. Particle fluxes associated with mesoscale eddies in the Sargasso Sea. *Deep-Sea Research II*, this issue [doi:10.1016/j.dsr2.2008.02.007].
- Chavanne, C., Flament, P., Lumpkin, R., Dousset, B., Bentamy, A., 2002. Scatterometer observations of wind variations by oceanic islands: implications for wind driven ocean circulation. *Canadian Journal of Remote Sensing* 28 (3), 466–474.
- Cherrier, J., Burnett, W.C., La Rock, P.A., 1995. Uptake of polonium and sulfur by bacteria. *Geomicrobiology Journal* 13, 103–115.
- Cherry, M., Heyraud, M., 1988. Polonium-210 in selected categories of marine organisms: interpretation on the basis of an unstructured marine food web model. In: Guary, J.C., Guegueniat, P., Pentreath, R.J. (Eds.), *Radionuclides: A Tool for Oceanography*. Elsevier Applied Science, Amsterdam, pp. 362–372.
- Cochran, J.K., Masqué, P., 2003. Short-lived U/Th series radionuclides in the ocean: tracers for scavenging rates, export fluxes and particle dynamics. *Reviews in Mineralogy and Geochemistry* 52, 461–492.
- Dickey, T., Nencioli, F., Kuwahara, V., Leonard, C., Black, W., Bidigare, R., Rii, Y., Zhang, Q., 2008. Physical and bio-optical observations of oceanic cyclones west of the island of Hawaii. *Deep-Sea Research II*, this issue [doi:10.1016/j.dsr2.2008.01.006].
- Ducklow, H.D., Steinberg, D.K., Buesseler, K.O., 2001. Upper ocean carbon export and the biological pump. *Oceanography* 14 (4), 50–58.
- Dugdale, R.C., Goering, J.J., 1967. Uptake of new and regenerated forms of nitrogen in primary productivity. *Limnology and Oceanography* 12, 196–206.
- Falkowski, P.G., Ziemann, D., Kolber, Z., Bienfang, P.K., 1991. Role of eddy pumping in enhancing primary production in the ocean. *Nature* 352, 55–58.
- Fisher, N.S., Burns, K.A., Cherry, R.D., Heyraud, M., 1983. Accumulation and cellular distribution of ^{241}Am , ^{210}Po and ^{210}Pb in two marine algae. *Marine Ecology Progress Series* 11, 233–237.
- Fowler, S.W., Knauer, G.A., 1986. Role of large particles in the transport of elements and organic compounds through the oceanic water column. *Progress in Oceanography* 16 (3), 147–194.
- Friedrich, J., Rutgers van der Loeff, M.M., 2002. A two-tracer (^{210}Po - ^{234}Th) approach to distinguish organic carbon and biogenic silica export flux in the Antarctic Circumpolar Current. *Deep-Sea Research I* 49, 101–120.
- Gardner, W.D., Richardson, M.J., Carlson, C.A., Hansell, D.A., Mishonov, A.V., 2003. Determining true particulate organic carbon: bottles, pumps and methodologies. *Deep-Sea Research II* 50, 655–692.
- Heyraud, M., Fowler, S.W., Beasley, T.M., Cherry, R.D., 1976. Polonium-210 in euphausiids: a detailed study. *Marine Biology* 34, 127–138.
- Ingalls, A.E., Liu, Z., Lee, C., 2006. Seasonal trends in the pigment and amino acid compositions of sinking particles in biogenic CaCO_3 and SiO_2 dominated regions of the Pacific sector of the Southern Ocean along 170°W . *Deep-Sea Research I* 53, 836–859.
- Jenkins, W.J., 1988. Nitrate flux into the euphotic zone near Bermuda. *Nature* 331, 521–523.
- Karl, D.M., Christian, J.R., Dore, J.E., Hebel, D.V., Letelier, R.M., Tupas, L.M., Winn, C.D., 1996. Seasonal and interannual variability in primary production and particle flux at Station ALOHA. *Deep-Sea Research II* 43, 539–568.
- Kim, G., Hussain, N., Church, T.M., 2000. Excess ^{210}Po in the coastal atmosphere. *Tellus* 52B, 74–80.
- Klaas, C., Archer, D.E., 2002. Association of sinking organic matter with various types of mineral ballast in the deep sea: implications for the rain ratio. *Global Biogeochemical Cycles* 16, 1116.
- Kuwahara, V.S., Nencioli, F., Dickey, T.D., Rii, Y.M., Bidigare, R.R., 2008. Physical dynamics and biological implications of cyclonic eddy *Noah* in the lee of Hawaii during E-Flux I. *Deep-Sea Research II*, this issue [doi:10.1016/j.dsr2.2008.01.007].
- Landry, M.R., Brown, S.L., Rii, Y.M., Selph, K.E., Bidigare, R.R., Yang, E.J., Simmons, M.P., 2008. Depth-stratified phytoplankton dynamics in Cyclone *Opal*, a subtropical mesoscale eddy. *Deep-Sea Research II*, this issue [doi:10.1016/j.dsr2.2008.02.001].
- La Rock, P., Hyun, J.H., Boutelle, S., Burnett, W.C., Hull, C.D., 1996. Bacterial mobilization of polonium. *Geochimica et Cosmochimica Acta* 60, 4321–4328.
- Laws, E.A., Falkowski, P.G., Smith, R.C., Ducklow, H., McCarthy, J.J., 2000. Temperature effects on export production in the open ocean. *Global Biogeochemical Cycles* 14, 1231–1246.
- Liu, Z., Stewart, G., Cochran, J.K., Lee, C., Armstrong, R.A., Hirschberg, D., Gasser, B., Miquel, J.-C., 2005. Why do POC concentrations measured using Niskin bottle collections sometimes differ from those using in-situ pumps? *Deep-Sea Research I* 52, 1324–1344.
- Lumpkin, C.F., 1998. Eddies and currents of the Hawaiian Islands. Ph.D. Dissertation. School of Ocean and Earth, Science and Technology, University of Hawaii at Manoa, Honolulu, 281pp.
- Mahaffey, C., Benitez-Nelson, C.R., Bidigare, R., Rii, Y., Karl, D.M., 2008. Nitrogen dynamics within a wind-driven eddy. *Deep-Sea Research II*, this issue [doi:10.1016/j.dsr2.2008.02.004].
- Maiti, K., Benitez-Nelson, C., Rii, Y.M., Bidigare, R.R., 2008. Influence of a mature cyclonic eddy on particle export in the lee of Hawaii. *Deep-Sea Research II*, this issue [doi:10.1016/j.dsr2.2008.02.008].
- Masqué, P., Sanchez-Cabeza, J.A., Bruach, J.M., Palacios, E., Canals, M., 2002. Balance and residence times of ^{210}Pb and ^{210}Po in surface waters of the northwestern Mediterranean Sea. *Continental Shelf Research* 22, 2127–2146.
- McGillicuddy Jr., D.J., Robinson, A.R., Siegel, D.A., Jannasch, H.W., Johnson, R., Dickey, T.D., McNeil, J., Michaels, A.F., Knap, A.H., 1998. Influence of mesoscale eddies on new production in the Sargasso Sea. *Nature* 394, 263–266.
- Murray, J.W., Paul, B., Dunne, J.P., Chapin, T., 2005. ^{234}Th , ^{210}Pb , ^{210}Po and stable Pb in the central equatorial Pacific: tracers for particle cycling. *Deep-Sea Research I* 52, 2109–2139.
- Nencioli, F., Dickey, T.D., Kuwahara, V.S., Black, W., Rii, Y.M., Bidigare, R.R., 2008. Physical dynamics and biological implications of a mesoscale cyclonic eddy in the lee of Hawaii: Cyclone *Opal* observations during E-Flux III. *Deep-Sea Research II*, this issue [doi:10.1016/j.dsr2.2008.02.003].
- Nozaki, Y., 1986. ^{226}Ra - ^{222}Rn - ^{210}Pb systematics in seawater near the bottom of the ocean. *Earth and Planetary Science Letters* 80, 36–40.
- Oschlies, A., 2001. Model-derived estimates of new production: new results point towards lower values. *Deep-Sea Research II* 48, 2173–2197.
- Paasche, E., 1980. Silicon content of five marine plankton diatom species measured with a rapid filter method. *Limnology and Oceanography* 25, 474–480.
- Patzert, W.C., 1969. Eddies in Hawaiian waters. *HIG Technical Report* 69-8. Hawaii Institute of Geophysics, University of Hawaii.
- Rii, Y., Brown, S., Nencioli, F., Kuwahara, V., Dickey, T., Karl, D., Bidigare, R.R., 2008. The transient oasis: nutrient-phytoplankton dynamics and particle export in Hawaiian lee cyclones. *Deep-Sea Research II*, this issue [doi:10.1016/j.dsr2.2008.01.013].
- Sarmiento, J.L., Toggweiler, J.R., 1984. New model for the role of the oceans in determining atmospheric pCO_2 . *Nature* 308 (5960), 621–624.
- Shimmie, G.B., Ritchie, G.D., Fileman, T.W., 1995. The impact of marginal ice zone processes on the distribution of ^{210}Pb , ^{210}Po and ^{234}Th and implications for new production in the Bellingshausen Sea, Antarctica. *Deep-Sea Research II* 42, 1313–1335.
- Siegel, D.A., McGillicuddy, D.J., Fields, E.A., 1999. Mesoscale eddies, satellite altimetry, and new production in the Sargasso Sea. *Journal of Geophysical Research—Oceans* 104 (C6), 13359–13379.
- Stewart, G.M., Fisher, N.S., 2003a. Experimental studies on the accumulation of polonium-210 by marine phytoplankton. *Limnology and Oceanography* 48 (3), 1193–1201.
- Stewart, G.M., Fisher, N.S., 2003b. Bioaccumulation of polonium-210 in marine copepods. *Limnology and Oceanography* 48 (5), 2011–2019.
- Stewart, G.M., Fowler, S.W., Teysse, J.-L., Cotret, O., Cochran, J.K., Fisher, N.S., 2005. Contrasting the transfer of polonium-210 and lead-210 across three trophic levels in the marine plankton. *Marine Ecology Progress Series* 290, 27–33.
- Stewart, G., Cochran, J.K., Xue, J., Lee, C., Wakeham, S.G., Armstrong, R.A., Masqué, P., 2007a. Exploring the use of ^{210}Po as a tracer of organic matter flux in the northwestern Mediterranean. *Deep-Sea Research I* 54, 415–427.
- Stewart, G.M., Masqué, P., Cochran, J.K., Miquel, J.C., Szlosek, J., Rodriguez, A.M., Fowler, S.W., Gasser, B., Hirschberg, D.J., 2007b. Comparing POC flux estimates from $^{210}\text{Po}/^{210}\text{Pb}$ water column profiles with estimates from sediment traps and $^{234}\text{Th}/^{238}\text{U}$ profiles, 0–200 m northwest Mediterranean. *Deep-Sea Research I* 54, 1549–1570.
- Sweeney, E.N., McGillicuddy, D.J., Buesseler, K.O., 2003. Biogeochemical impacts due to mesoscale eddy activity in the Sargasso Sea as measured at the Bermuda Atlantic Time-series Study (BATS). *Deep-Sea Research II* 50, 3017–3039.
- Verdeny, E., Masqué, P., Garcia-Orellana, J., Hanfland, C., Cochran, J.K., Stewart, G.M., 2008. POC export from ocean surface waters by means of $^{234}\text{Th}/^{238}\text{U}$ and $^{210}\text{Po}/^{210}\text{Pb}$ disequilibria: a review of the use of two radiotracer pairs. *Deep-Sea Research II*, in revision.
- Volk, T., Hoffert, M.I., 1985. Ocean carbon pumps: analysis of relative strengths and efficiencies in ocean-driven atmospheric CO_2 changes. In: Sundquist, E.T., Broecker, W.S. (Eds.), *The Carbon Cycle and Atmospheric CO_2 : Natural Variations Archean to Present*. Geophysics Monograph Series 32. AGU, Washington, DC, pp. 99–110.
- Waples, J.T., Benitez-Nelson, C.R., Savoye, N., Rutgers van der Loeff, M., Baskaran, M., Gustafsson, Ö., 2006. An introduction to the application and future use of ^{234}Th in aquatic systems. *Marine Chemistry* 100, 166–189.
- Williams, R.G., Follows, M.J., 2003. Physical transport of nutrients and the maintenance of biological production. In: Fasham, M. (Ed.), *Ocean Biogeochemistry: The Role of the Ocean Carbon Cycle in Global Change*. Springer, pp. 19–51.